Palaeogeography, Palaeoclimatology, Palaeoecology 490 (2018) 131–140

Contents lists available at ScienceDirect

Palaeogeography, Palaeoclimatology, Palaeoecology

journal homepage: www.elsevier.com/locate/palaeo

Photosynthetic pathway of grass fossils from the upper Miocene Dove Spring Formation, Mojave Desert, California

Hannah M. Liddy[a,*], Sarah J. Feakins[a,**], Frank A. Corsetti[a], Rowan Sage[b], Nancy Dengler[b,1], David P. Whistler[c], Gary T. Takeuchi[d], Mark Faull[e], Xiaoming Wang[a,c]

[a] Department of Earth Science, University of Southern California, Los Angeles, CA 90089, USA
[b] Department of Ecology and Evolutionary Biology, University of Toronto, Toronto, ON M5S3B2, Canada
[c] Department of Vertebrate Paleontology, Natural History Museum of Los Angeles County, Los Angeles, CA 90007, USA
[d] Department of Rancho La Brea, La Brea Tar Pits and Museum, Los Angeles, CA 90036, USA
[e] Red Rock Canyon State Park, California State Parks, Tehachapi, CA 93581, USA

ARTICLE INFO

Keywords:
C_3
C_4
Carbon isotopes
Grassland
Grass anatomy

ABSTRACT

The spread of grasslands in the Miocene and of C_4 grasses in the late Miocene-Pliocene represents a major development in terrestrial plant evolution that affected the climate system and faunal evolution. The macrofossil record of grasses is sparse, likely due to the limited preservation potential of grasses. Diagnosis of the C_3 or C_4 photosynthetic pathway depends on preservation of both cellular structures and organic carbon for isotope analysis. Here we analyze the anatomical and isotopic composition of newly-collected grass fossils from the Dove Spring Formation, Red Rock Canyon State Park, California, USA, located in the El Paso Basin on the western side of the Basin and Range Province, a site previously identified as one of the earliest known C_4 grass fossil bearing localities. We analyzed the anatomical and geochemical characteristics of these new grass fossils dated to 12.01–12.15 Ma. The fossils analyzed in this study include grass shoots and in cross-section display anatomy indicative of the C_3 photosynthetic pathway. We isolated organic carbon from the stem fossils and determined the carbon isotopic composition to be -24.8 ± 0.5‰. Together, the anatomical and geochemical analyses confirm that these plants used the C_3 photosynthetic pathway. Our findings are consistent with dietary evidence based on tooth enamel from grazing mammals of available C_3 resources in the same sections. These newly reported Miocene-age C_3 grass fossils contribute to a sparse macrofossil record of grass evolution. Overall, paleoecological reconstructions at this site indicate more humid conditions during the Miocene compared to the modern Mojave Desert with C_3 grasses and diverse grazing mammals.

1. Introduction

The family of grasses (Poaceae) is highly diverse with up to 11,000 species and largely dominates open habitat ecosystems around the world (Gibson, 2009). Within grasses, a specialized photosynthetic pathway for fixating CO_2 from the atmosphere evolved relatively recently. This pathway, known as C_4 photosynthesis, is an adaptation to the ancestral C_3 photosynthetic pathway that acts to mitigate the effects of photorespiration that can occur in response to ecological pressures in C_3 photosynthesis. C_4 has evolved at least 62 different times, resulting in one of the best examples of convergent evolution (Sage et al., 2011, 2012). The vast majority of C_4 origins appear to have occurred after a precipitous drop in atmospheric CO_2 in the Oligocene ca. 30 Ma based on molecular clock evidence (Christin et al., 2008, 2014; Vicentini et al., 2008), however incorporation of microfossil data indicate an earlier C_4 origin in the grass subfamily Chloridoideae to ~41 Ma when atmospheric CO_2 was still high (Christin et al., 2014; Prasad et al., 2011). Despite these early estimates, the macrofossil record of grasses is limited as a result of the often arid, well-drained environments where grasses grow, where if grasses become buried, are often destroyed by oxidation (Cerling, 1999; Retallack, 1990). As a result, the macrofossil record of grasses is exceedingly rare and can be hampered by taphonomic alteration.

C_4 grasses are both anatomically and biochemically distinct from C_3 grasses. In C_3 plants, both carbon assimilation and carbon reduction occur in the mesophyll cells. In C_4 plants, these processes are spatially

* Correspondence to: H.M. Liddy, Center for Climate Systems Research, Columbia University, New York, NY 10025, USA.
** Corresponding author.
E-mail addresses: hl3147@columbia.edu (H.M. Liddy), feakins@usc.edu (S.J. Feakins).
[1] Professor Emeritus.

http://dx.doi.org/10.1016/j.palaeo.2017.10.019
Received 12 January 2017; Received in revised form 13 October 2017; Accepted 17 October 2017
Available online 20 October 2017
0031-0182/

separated resulting in the internal concentration of CO_2, where CO_2 is assimilated into mesophyll cells and then shuttled into vascular bundle sheath cells where carbon reduction occurs via the Calvin cycle (Hatch, 1987). The biochemical compartmentalization of C_4 photosynthesis commonly results in a wreath-like structure, when viewed in cross section, known as "Kranz" anatomy in which mesophyll cells wrap around an inner layer of bundle sheath cells (Brown, 1975; Hatch, 1987). Almost all known C_4 plant lineages have Kranz anatomy (Bowes, 2011; Sage et al., 2011; Voznesenskaya et al., 2001). The ability of the C_4 pathway to concentrate CO_2 around the photosynthetic enzyme, Rubisco, confers a competitive advantage over the C_3 photosynthetic pathway in warm, dry and/or low CO_2 conditions (Ehleringer et al., 1997). As a result of this process, the organic carbon isotope value of C_4 plants is more ^{13}C-enriched than co-occurring C_3 plants. Therefore both visual as well as isotopic evidence can be used to distinguish between the C_3 and C_4 photosynthetic pathway.

Few sites offer both anatomical evidence of the photosynthetic pathway as well as isotopic evidence. Grass fossils from the Middle Miocene (~14 Ma) were found at the Fort Ternan Formation in Kenya (Dugas and Retallack, 1993; Retallack, 1992). Although internal anatomy was not preserved, the cuticle morphology was compared with extant species of both C_3 and C_4 grasses in an assemblage more comparable to African grasslands at 2–3 km elevation than modern lowland C_4-dominant savannas. (Dugas and Retallack, 1993; Retallack et al., 1990). The carbon isotopic value of paleosols from that locality further indicate a C_3-dominated environment supporting that C_4 grasses, if present, were not abundant (Cerling et al., 1991). Grass fossils from the western Mojave Desert, California, from the Ricardo Formation (now Dove Spring Formation) of the El Paso Basin were initially interpreted as Pliocene-age and later revised as late Miocene-age based on fossil assemblages and new radiometric dates (Nambudiri et al., 1978; Tidwell and Nambudiri, 1989). These fossils were reported to have Kranz anatomy and small interveinal distances indicative of C_4 photosynthesis (Nambudiri et al., 1978) and were later reported in detail in Tidwell and Nambudiri (1989). A $\delta^{13}C$ value of −13.7‰ was obtained for bulk carbon within the fossil and the interpretation was that they used the C_4 pathway (Tidwell and Nambudiri, 1989). Additional grass fossils that lacked Kranz anatomy and yielded a $\delta^{13}C$ value −24.6‰ were also reported (Nambudiri et al., 1978). A subsequent study described C_3 grass fossils from Sperry Wash, located in southeastern California south of Death Valley, 180 km away, in detail (Tidwell and Nambudiri, 1990). These fossils were surficially collected from eroded strata spanning the latest Miocene (5.4 ± 0.2 Ma) based on radiometric dating to late Pliocene/early Pleistocene-age strata based on stratigraphic relationships. A third late Miocene grass fossil has been reported from the Ogallala Formation (7–5 Ma) in northwestern Kansas (Thomasson et al., 1986). The grass fossil was inferred to be C_4 based on the presence of Kranz anatomy. The fossils were assessed to be completely permineralized and carbon isotopic measurements were not attempted (Thomasson et al., 1986). This amounts to a sparse fossil record of C_4 grass fossils.

In order to investigate the presence of late Miocene grasses via anatomical and isotopic evidence, we revisited the grass fossil site in the Dove Spring Formation (formerly Ricardo Formation), located in the western Mojave Desert, California (Nambudiri et al., 1978; Tidwell and Nambudiri, 1989). We found additional grass fossils from two stratigraphic locations that allow us to securely date these new fossils to the upper Miocene. The anatomical description and isotopic composition of these newly-collected grass macrofossil samples are the focus of this study and provide the means to diagnose the photosynthetic pathway by the same criteria applied to modern plants.

1.1. C_4 versus C_3 anatomy

As a result of convergent evolution, there is a high degree of diversity in C_4 leaf anatomy and biochemical characteristics (Freitag and Stichler, 2000; Kadereit et al., 2003; Muhaidat et al., 2007; Voznesenskaya et al., 2001), however, there are commonalities among C_4 plants. Three main properties are used to distinguish C_4 species from C_3 species (Dengler and Nelson, 1998; Edwards et al., 2001; Leegood, 2002; Lundgren et al., 2014; Sage, 2016). One requirement for C_4 photosynthesis is the specialization of two specific photosynthetic cell types resulting in the differentiation between where carbon is assimilated and where it is fixated via the Calvin Benson cycle. The first compartment (mesophyll cells) is more exposed to regions of intercellular airspace and houses the PEP-C reactions, and the second compartment (typically bundle sheath cells) limits the loss of CO_2 and HCO_3 and is the location of the Calvin Cycle reaction. A second requirement is the close contact of these two regions to facilitate the rapid diffusion of metabolites, which is commonly achieved via high vein density or, more precisely, low ratios of mesophyll to bundle sheath cells as cell size and orientation can differ due to taxonomic variation (Christin and Osborne, 2014; Hattersley and Watson, 1975; Sinha and Kellogg, 1996). Generally, interveinal distance in C_4 plants ranges between 60 and 150 μm and one to four mesophyll cells, while in C_3 plants, interveinal distance is > 200 μm and more than five mesophyll cells (Dengler et al., 1994; Ogle, 2003). In C_3 plants this anatomy can be similarly achieved to address physiological demands such as the transport of metabolites or leaf hydraulics (Sack and Scoffoni, 2013; Sack et al., 2012), which can complicate the exclusive identification of the C_4 photosynthetic type via this anatomical property (Christin et al., 2013; Lundgren et al., 2014; Muhaidat et al., 2007). A third requirement is the presence of abundant chloroplasts in the second compartment, which is typically achieved via the enlargement of the bundle sheath cells to accommodate an increase in the number of chloroplasts. It is also possible to achieve the same ends via an increase in the amount of bundle sheath tissue such that the volume of bundle sheath cells relative to mesophyll cells can be quantitatively constrained in C_4 plants (Dengler et al., 1994; Hattersley, 1984; Muhaidat et al., 2007). The anatomical aspects of these requirements for C_4 function are referred to as Kranz anatomy. Given the diversity in anatomical traits, carbon isotope analysis can be a critical way of identifying the use of the C_4 pathway, especially in fossil grasses where the preservation may be limited to lignified structures.

2. Stratigraphic context

2.1. Geologic setting

The fossil-bearing Dove Spring Formation is located within the El Paso Basin at the western end of the Basin and Range Province and is bounded to the west by the Sierra Nevada (Fig. 1A). Uplift of the El Paso Mountains along the El Paso Fault exposed > 6.2 km of sedimentary and volcanic rock. The Ricardo Group is divided into two Miocene-age formations: the Cudahy Camp Formation comprised of 450 m of dominantly volcanic rocks and the Dove Spring Formation comprised of 1800 m of fluvial, lacustrine and volcanic rocks (Dibblee, 1952; Loomis and Burbank, 1988). The Dove Spring Formation lies disconformably over the Cudahy Camp Formation, and Quaternary deposits originating from the Sierra Nevada lie unconformably over the Dove Spring Formation (Whistler et al., 2009).

The Dove Spring Formation, divided into six members spanning ~8–12.5 Myr, was deposited in an elongate, fault-bound trough (Loomis and Burbank, 1988; Whistler et al., 2009). The sedimentary and volcanic fill consists of conglomerate, sandstone, mudstone, chert, basalt, and tuff. Specifically, five major paleoenvironments are identified including (1) fine-grained lacustrine deposits, (2) coarse-grained fluvial deposits of channel sandstone and channel conglomerates, (3) finer-grained overbank and floodplain silts, (4) poorly sorted alluvial fan deposits, and (5) paleosol caliche and silicified hardpan deposits (Whistler et al., 2009; Whistler and Burbank, 1992). These sedimentary deposits contain a diverse fossil assemblage of at least 86 species of

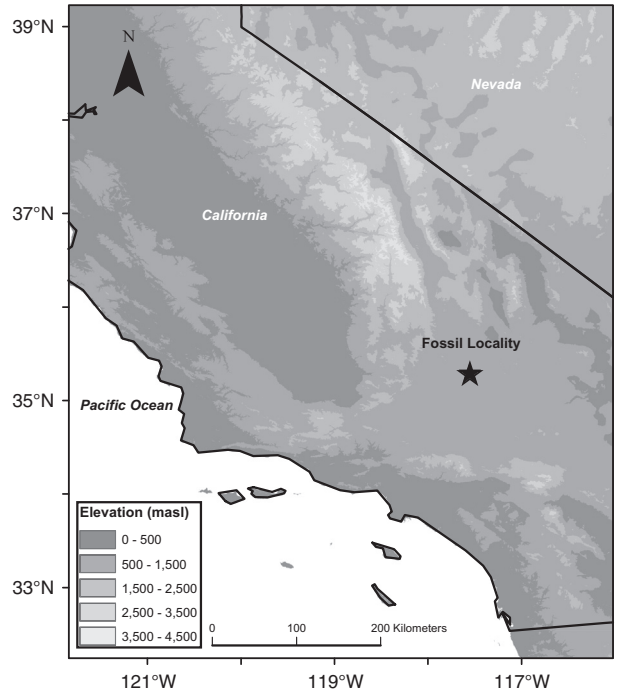

Fig. 1. Regional map of the fossil locality (star) at Red Rock Canyon, California, USA.

fossil vertebrates that are Clarendonian though earliest Hemphillian-aged (Merriam, 1919; Tedford et al., 1987; Wood et al., 1941).

The fluvial and lacustrine rock sequence of the Dove Spring Formation was deposited by ephemeral braided streams draining into a semi-permanent lake in the center of a broad basin (Loomis and Burbank, 1988; Whistler et al., 2009). In the lower part of the formation, paleocurrent orientation is preferentially directed toward the north-northwest suggesting a source to the south from the uplifted Mojave block (Loomis and Burbank, 1988). At ~10 Ma with the initiation of sinistral shear on the Garlock fault, the El Paso Basin began to rotate counter clockwise, and by 9 Ma, basin and range style extension began in this region (Burbank and Whistler, 1987; Loomis and Burbank, 1988). In the upper strata of the formation (Members 5 and 6), paleocurrent evidence is sparse and a transition in lithology to coarser clast sandstones and conglomerates is interpreted to be poorly-sorted alluvial fan deposits indicative of a Sierra Nevada detrital source (Loomis and Burbank, 1988) (Fig. 1C). Within these uppermost sections (upper 200 m), well-developed paleosol, caliche and silicified hardpan deposits indicate a shift to more arid conditions in the basin at this time (Whistler et al., 2009). Throughout the Dove Spring Formation, the sedimentary fill is punctuated by pyroclastic and basaltic volcanic flows, which provide material for radiometric dating of the Dove Spring Formation sequence (Bonnichsen et al., 2008; Cox and Diggles, 1986; Perkins et al., 1998; Perkins and Nash, 2002; Smith et al., 2002; Whistler et al., 2009).

2.2. Tephra and biostratigraphic age control

A total of 18 volcanic air-fall vitric ashes have been mapped throughout the Dove Spring Formation (Whistler et al., 2009). Active volcanism was occurring in the southern Great Basin and the Yellowstone 'Hot Spot' in the late Miocene (Bonnichsen et al., 2008; Perkins et al., 1998; Perkins and Nash, 2002). Two basalt flow sequences, each including several individual flows, are sourced south of the Garlock Fault in the Lava Mountains (Monastero et al., 1997; Smith et al., 2002). The radiometric dates span 12.15 ± 0.04 Ma (Cougar Point Tuff V in Member 2) to 8.5 ± 0.15 Ma (near the top of the formation in Member 6) (Perkins et al., 1998; Bonnichsen et al., 2008; Whistler and Burbank, 1992) (Fig. 1C). The oldest volcanic strata that provide the most basal age constraint for the Dove Spring Formation is dated to 12.15 ± 0.04 Ma followed by the Ibex Hollow tephra dated to 12.01 ± 0.03 Ma (Perkins and Nash, 2002; Whistler et al., 2009).

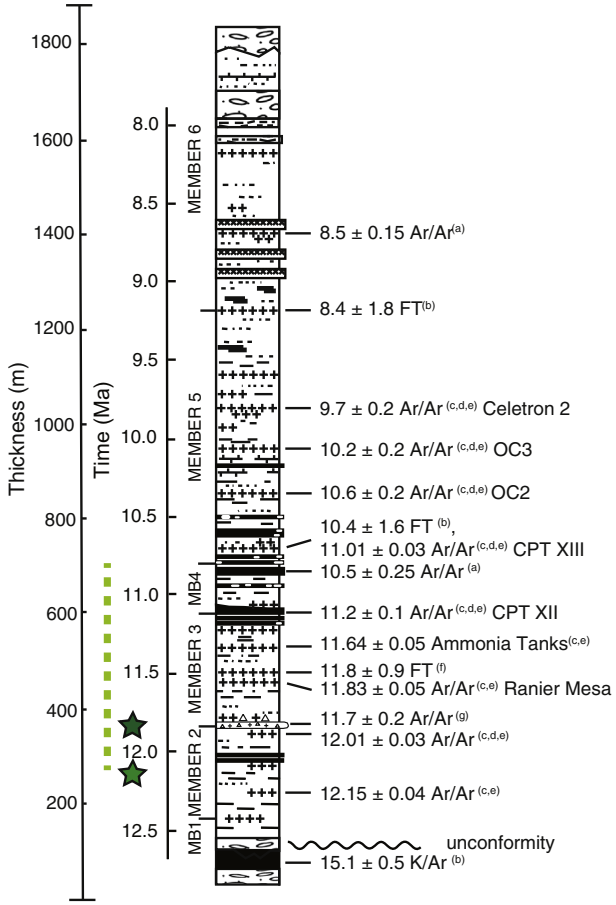

Fig. 2. Stratigraphic section of the Dove Spring Formation modified from Whistler and Burbank, 1992 with ages updated from Whistler et al., 2009. The age chronology includes dating methods such as fission track ((b) Cox and Diggles, 1986; (f) Loomis and Burbank, 1988), Ar/Ar radiometric dates ((e) Bonnichsen et al., 2008; (c) Perkins et al., 1998; (d) Perkins and Nash, 2002; (g) Smith et al., 2002; (a) Whistler and Burbank, 1992), K/Ar radiometric dates ((b) Cox and Diggles, 1986), and biostratigraphic correlations ((e) Bonnichsen et al., 2008; (c) Perkins et al., 1998). The green stars delineate the approximate stratigraphic position of the two fossil localities of the grass fossils reported in this study. The dashed green line represents the estimated stratigraphic range from where the previously reported C_4 grass fossils were collected in Nambudiri et al. (1978). (For interpretation of the references to colour in this figure legend, the reader is referred to the web version of this article.)

2.3. Sample collection

We revisited the Red Rock Canyon fossil locality that has yielded a fossil grass thought to be the oldest known C_4 grass fossil (Nambudiri et al., 1978). The fossil was reported from the Ricardo Formation (now Dove Spring Formation) in the Last Chance Canyon, which refers broadly to a large watershed within the El Paso Mountains of eastern Kern County, California. Unfortunately, the precise stratigraphic location of the Nambudiri et al. (1978) fossil is unknown, but is reported to have been collected from a locality within Members 4 and 5 (as named by Dibblee, 1952 and later updated to mid-Member 2 to Member 4 by Loomis and Burbank, 1988), which spans an age range of ~12–11 Ma (Loomis and Burbank, 1988; Tidwell and Nambudiri, 1989, Whistler et al., 2009) (Fig. 2). The first grass fossil herein described, Natural History Museum of Los Angeles County (LACM) 155,204, was surficially collected by a volunteer from just above the Ibex Hollow tephra

dated to 12.01 ± 0.03 Ma (Bonnichsen et al., 2008; Perkins et al., 1998; Perkins and Nash, 2002) at LACM locality 3679. The second group of fossils was recovered from the LACM locality 8019, Member 2 of the Dove Spring Formation. This locality lies between two ash layers: below the Ibex Hollow tephra dated to 12.01 ± 0.03 Ma (Bonnichsen et al., 2008; Perkins et al., 1998; Perkins and Nash, 2002) and in proximity to the Cougar Point Tuff V dated to 12.15 ± 0.04 Ma (Bonnichsen et al., 2008; Perkins et al., 1998; Whistler et al., 2009). Three of the thin sections that were catalogued and housed in the Department of Vertebrate Paleontology, LACM are reported here: LACM 160024, LACM 160025, LACM 160026. Two additional hand samples were collected but did not yield viable thin section images for anatomical analysis.

3. Methods

3.1. Fossil imaging

The surficially collected grass fossil was imaged using light microscopy (Zeiss Imager M2 m with a Zeiss Axiocam MRc) at USC. For depth of field issues, some images were taken using a KEYENCE VH-Z100R Real Zoom Lens with magnification range of ×100–×1000 optical microscopy at the LACM.

All field-excavated samples were cut with a rock saw to hand-sample size to reveal as many leaf stems in cross section as possible. Surfaces were polished to identify well-preserved stems. Thin sections were prepared to 7.62 cm × 5.08 cm with 30 μm thickness and clear epoxy (by Wagner Petrographics, Lindon, Utah). Thin section samples were analyzed using light microscopy (Zeiss Imager M2 m with a Zeiss Axiocam MRc) at USC and images prepared with MOSAIC software to reveal the internal anatomy of the fossil leaves on features larger than single microscope images.

3.2. Organic carbon isotopic measurements

To minimize exposure to modern contamination, field-excavated samples were cut with a rock saw to remove weathered surfaces and veins. The pieces were then broken apart to separate fossils from the matrix in a jaw crusher that was cleaned of possible organic material using igneous rock blanks. These smaller pieces were then dissolved in dilute (10%) HCl until bubbling stopped to remove any remaining rock matrix surrounding the fossilized stems. Silicified grass stems were powdered in a solvent-rinsed ball mill, and the matrix was drilled to powder. Up to 5 g of sediment was added to 40 mL of 1 M hydrochloric acid and heated to 70 °C in a water bath for 4 h to remove carbonates including calcite as well as more refractory carbonate phases (e.g., dolomite) (Brodie et al., 2011; Galy et al., 2007; Ward et al., 2007). Samples were rinsed with deionized water three times then dried in a drying oven at 50 °C for 24 h. The low total organic carbon (TOC) content of the samples and matrix required sample sizes of 257–308 mg that were measured into Sn capsules. The TOC and isotopic composition of organic carbon ($\delta^{13}C_{org}$) was determined using a Costech Elemental Combustion System (EA 4010) connected to a Picarro cavity ring down spectrometer (G2131-i) via a Picarro Liaison (A0301). Two blanks and two standards (USGS-40 [Glutamic Acid]$\delta^{13}C_{org} = -26.6‰$) and bulk calcite ($\delta^{13}C_{org} = -37.9‰$) were run in replicate at the beginning and end of the sample run to standardize measurements to the Vienna Pee Dee Belemnite (VPDB)-Lithium carbonate standard prepared by H. Svec (LVSEC) isotopic scale. $\delta^{13}C_{org}$ values are reported using delta notation in per mil (‰) units relative to the VPDB-LVSEC isotopic scale. Replicate standard precision was better than 0.23‰, and values were within 0.24‰ of known values. Standards were diluted with kaolinite to test reproducibility when measuring low TOC materials, with reproducibility of these large mass aliquots within 0.6‰. Replicates of different aliquots of the matrix and stem sample were reproducible to within 0.37‰.

3.3. Inorganic carbon isotopic measurements

The rock matrix of the embedded plant material was drilled to powder. Of this powder, ~12 mg was weighed into 10 mL glass Exetainer vials with rubber septa caps. Vials were evacuated and pre-acidified with 1 mL 30% H_3PO_4. Samples and standards were heated for 80 min in a water bath at 70 °C to ensure that all carbon associated with more refractory phases (e.g. dolomite) were released as CO_2. Samples were run on a Picarro CRDS coupled to an Automate preparative device. Two blanks and two standards (USGS-40 [Glutamic Acid] $\delta^{13}C = -26.4‰$) and bulk calcite ($\delta^{13}C = 2.47‰$) were run in replicate at the beginning and end of the sample run to standardize measurements to the VPDB-LVSEC isotopic scale. Replicate standard precision was better than 0.022‰, and values were within 0.000067‰ of known values.

4. Results

4.1. Plant fossil descriptions

LACM 155204 consists of 12 shoots borne on a partial rhizome (Fig. 3A, B). Shoot diameters range from ~2–3 mm. The abaxial leaf epidermis displays small diameter ridges and furrows, corresponding to grass leaf epidermal cells (Fig. 4C). Internal anatomy was best preserved in the shoot marked by a star in Fig. 3B, and the following descriptions of LACM 155204 are based on those features.

The central culm of the marked shoot of LACM 155204 is surrounded by one complete and one partial leaf (Fig. 4A). The culm is oval-shaped with a diameter of 1.2 × 1.8 mm. Large vascular bundles protrude into a hollow pith. Smaller vascular bundles appear within the parenchymatous ground tissue between the larger bundles. Strands of sclerenchyma tissue are present within the hypodermal region (Fig. 4D). Large vascular bundles within the culm are oval-shaped with dimensions of ~150 × 200 μm (Fig. 5A, D). Within the large vascular bundles, a semi-circular region of phloem is present toward the exterior of the stem (Fig. 5A, B). Two circular metaxylem elements flank the sides of the bundles, and in some bundles, a third metaxylem element is preserved in the center of the bundle (Fig. 5B) A region of protoxylem parenchyma cells is present toward the interior of the culm. A single layer of bundle sheath cells that are 7–10 μm in diameter can be distinguished (Fig. 5B, C). The complete leaf that encircles the culm has a smooth outline and widely spaced vascular bundles, suggesting that the section passes through the basal sheath of the leaf (Fig. 4A, B). Smaller vascular bundles within the leaf sheath have diameters of ~45 × 60 μm and are spaced ~300 μm apart. Metaxylem and protoxylem are distinguishable within one of these bundles (Fig. 4D).

Grass shoots were abundant in the excavated hand samples; however, anatomical preservation was limited (Fig. 3C). Each sample represents a subsample of the specimens collected in the field as preservation of internal structures varied between the hand samples. In general, the permineralized plant fossils LACM 160026, LACM 160025, and LACM 160024 are likely from the Poaceae family. Each specimen appears to represent a grass shoot with a central culm region surrounded by one or more concentrically arranged leaves in cross section. Shoots range from 2.4 to 4.4 mm in diameter.

LACM 160026 is approximately 3.75 mm in diameter (Fig. 6A). Two leaves surround a central area of parenchymatous tissues, most likely representing culm. In the innermost leaf, the midvein is well-preserved within a thickened midrib region. The midvein is approximately 500 μm in diameter with a single layer of bundle sheath cells and internal vascular tissue. Only one smaller vein is preserved in this leaf. In contrast, the outermost leaf, while altered by taphonomy, displays large-scale ridges and grooves, indicative that this leaf has been sectioned through the blade region. Smaller vascular bundles can be distinguished opposite some of the ridges. Smaller vascular bundles are ~200 μm in diameter and are spaced ~5 mm apart (although this

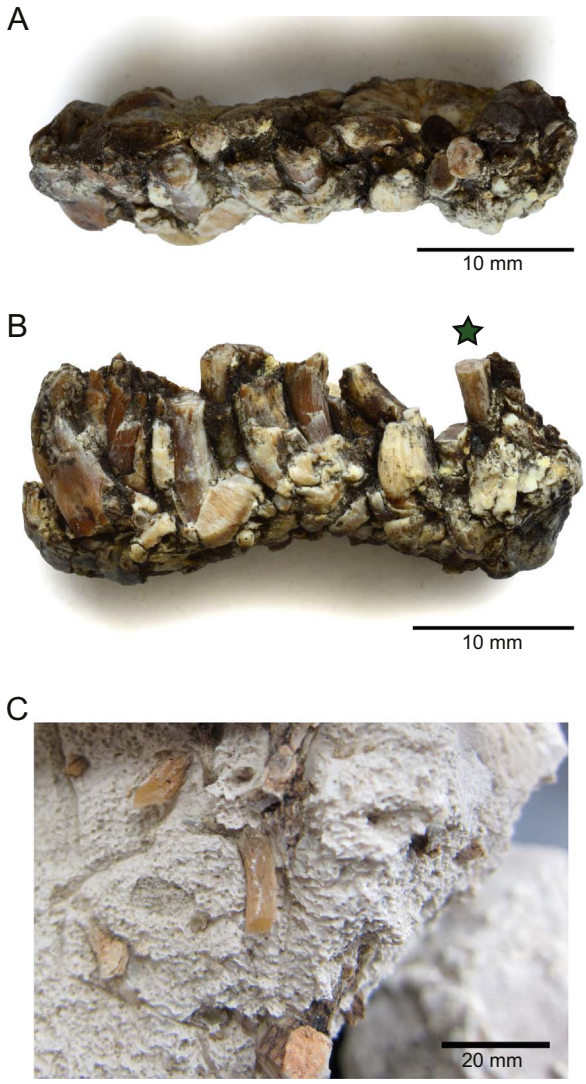

Fig. 3. (A) Top view of grass fossil stems, LACM 155204, collected from LACM locality 3679. (B) Side view of the same grass fossil stems, LACM 155204. Star marks shoot illustrated in Figs. 3 and 4. (C) Fossil plant embedded hand sample collected from LACM locality 8019.

distance is likely a reflection of what is preserved after permineralization).

LACM 160025 has similar anatomy to LACM 160026 (Fig. 6B). The sample is less symmetrical with approximate diameters of 4.4 × 2.4 mm. The parenchymatous region at the center likely represents the culm. The innermost leaf has a prominent midvein 500 μm in diameter positioned within a thickened midrib. Smaller vascular bundles located within the leaf are ~200 μm in diameter and spaced approximately 1.5 mm apart. Although the preservation is less clear, a second leaf with conspicuous smaller vascular bundles is present. The smaller vascular bundles are of comparable size to those observed in LACM 160026.

Much of the internal structure of LACM 160024 was not preserved (Fig. 6C). However, recognizable features seem to be similar to LACM 160026 and LACM 160025. While the internal features of the central culm were not preserved, well-preserved vascular bundles occur within flattened organs that may represent leaf sheaths surrounding a culm. The diameters of the smaller vascular bundles were comparable to their counterparts (200 μm) in LACM 160026 and LACM 160025. However, some smaller bundles are observed with diameters of 150 μm. The inset in Fig. 6C shows two compressed leaves with several smaller vascular bundles; one of these shows two bundle sheath layers: an inner mestome sheath (125 × 185 μm) and an outer parenchymatous bundle sheath (200 × 175 μm). The inset in Fig. 6C shows two compressed leaves with several smaller vascular bundles. One of these shows two bundle sheath layers: an inner sheath with cells of 13 μm in diameter and an outer sheath with cells of 20 μm in diameter. Internal features of vascular bundles such as metaxylem elements are not preserved. The spacing between vascular bundles ranges from 200 to 450 μm and is less than in other samples, possibly the result of taphonomic alteration.

4.2. Stable carbon isotopes

The stable carbon isotope value of the fossil material and surrounding matrix of the hand samples are listed in Table 1. The fossil material and surrounding matrix had low TOC values of 0.001% and 0.003%, respectively. The $\delta^{13}C_{org}$ value of the grass fossil is −24.4 ± 0.03‰, and the $\delta^{13}C_{org}$ value of the matrix $\delta^{13}C_{org}$ is −27.3 ± 0.42‰. The rock matrix is significantly more negative than the fossil material ($p < 0.01$), which suggests that the organic carbon from the fossil is not contaminated by the organic carbon of the matrix. The total inorganic carbon (TIC) content of the matrix is 7.75% and the $\delta^{13}C$ value is −3.79 ± 0.05‰.

Two other hand samples had imbedded fossilized plant material but did not yield viable thin section images. The $\delta^{13}C_{org}$ value of these plant fossils is −25.3 ± 0.03‰ and −24.6 ± 0.5‰, and the matrix $\delta^{13}C_{org}$ value is −26.9 ± 0.34‰ and −31.3 ± 0.89‰ (1σ, $n = 3$), respectively. The matrix is also significantly more negative than the fossil material ($p < 0.01$), which suggests that the organic carbon from the fossil is not contaminated by the organic carbon of the matrix. The TIC content of the matrix is 10.2% and 9.06% and the $\delta^{13}C$ value is −4.97 ± 0.02‰ and −4.27 ± 0.05‰.

5. Discussion

5.1. Grass fossils from the Dove Spring Formation

We revisited the locality of the oldest known C_4 grass fossil from Red Rock Canyon State Park, California, USA to recover additional grass fossils. Grass fossils were not ubiquitous throughout the Dove Spring Formation, and a search for additional fossils yielded only the material presented in this study. Most of the structures preserved are lignified sections of whole shoots, and the preservation of photosynthetic tissues was limited. Of the three anatomical hallmarks for C_4 photosynthesis, we found some evidence for bundle sheath layers surrounding smaller veins. The diameters of both inner and outer sheath cells fell within the range for both C_3 and C_4 PACMAD grass species (Christin et al., 2013). Preserved veins were separated by distances 300 μm or more, well above the range for C_4 grasses (Dengler et al., 1994). A third hallmark, increase in number and size of chloroplasts, was not preserved in this material. Thus, our anatomical observations showed no positive evidence for C_4 Kranz anatomy. Therefore, we infer that the plant fossils reported here are likely C_3 grass shoot cross-sections from the Poaceae family. No additional C_4 grass fossils were recovered from this locality.

5.2. Miocene carbon isotope values and organic carbon content

The grass fossils reported in this study have a mean $\delta^{13}C$ value of −24.8 ± 0.5‰, which indicates the use of the C_3 photosynthetic pathway based on the range of modern C_3 plants (Cerling and Harris, 1999; Tipple and Pagani, 2007). However, the carbon isotopic composition of plant material reflects both the photosynthetic pathway used by the plant to fix carbon dioxide from the atmosphere as well as the carbon isotopic composition of atmospheric carbon dioxide (Farquhar et al., 1989), which has varied across geological time. The late Miocene average $\delta^{13}C$ of atmospheric CO_2 reconstructed from the $\delta^{13}C$ values of

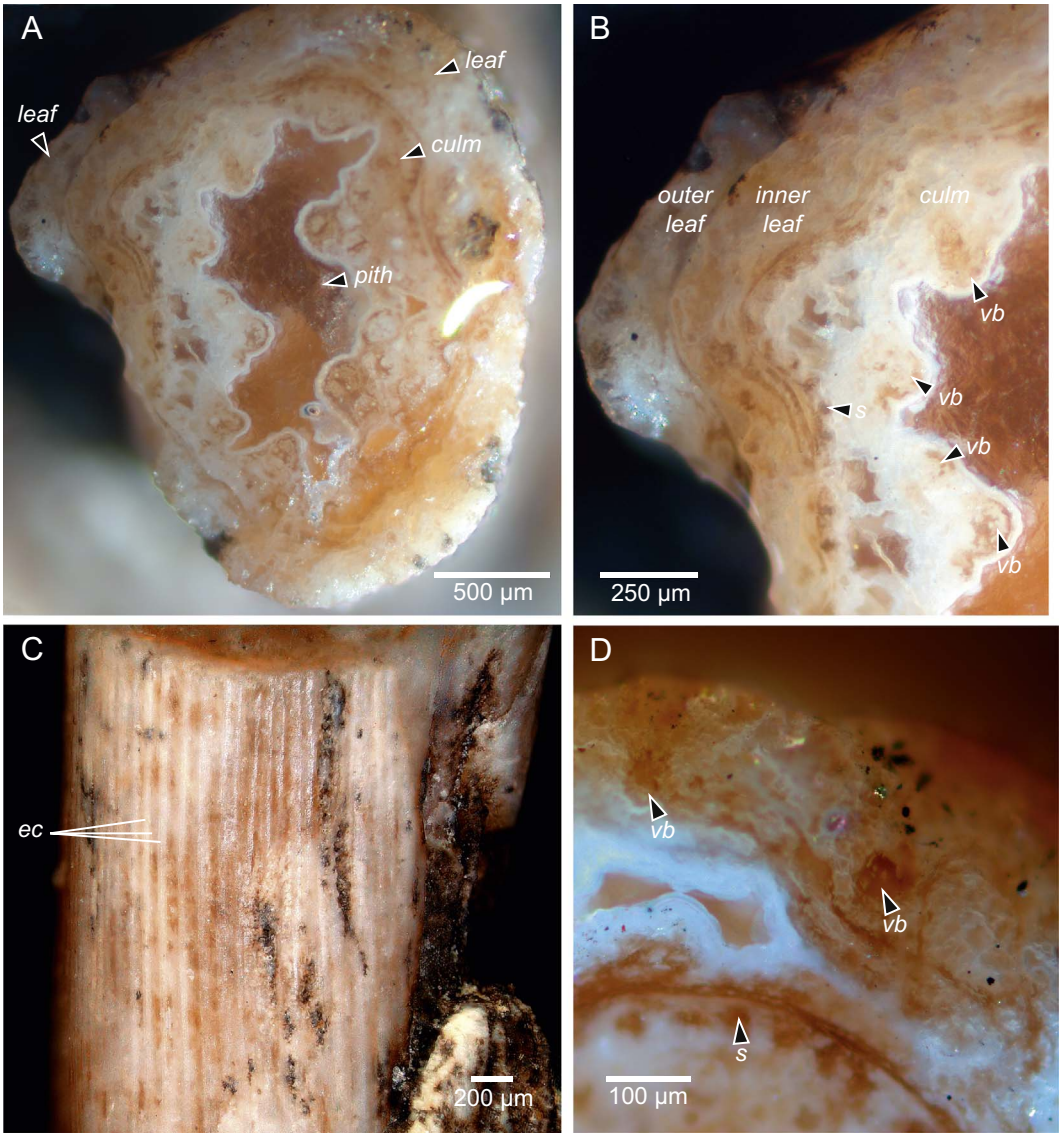

Fig. 4. Cross-section and longitudinal images of LACM 155204. (A) Cross section of culm and pith with surrounding leaf sheaths and vascular bundles protruding into the hollow culm. (B) Inner and outer leaves surrounding the culm. Vascular bundles (*vb*) protrude into the hollow pith. Sclerenchyma tissue(*s*) line the outer edge of the culm. (C) Longitudinal view of the culm with ridges and furrows that make up the grass leaf epidermal cells (*ec*). (D) Two vascular bundles (*vb*) in the inner sheath. Strands of sclerenchyma tissue (*s*) line the abaxial side of the epidermis for structural support.

benthic foraminifera from North Atlantic ODP Sites 553, 558, 563, and 601 is −6.0 ± 0.2‰ (maximum = −5.4‰ and minimum = −6.5‰) (Tipple et al., 2010). Other reconstructions of the $\delta^{13}C$ of CO_2 based on planktonic foraminifera come to similar conclusions with values varying between −5.0‰ to −6.2‰ (Passey et al., 2002). Therefore, the Miocene $\delta^{13}C$ of CO_2 was on average higher than pre-industrial (−6.5‰) (Friedli et al., 1986) and modern (−8.5‰, 2015) (Keeling et al., 2001). Assuming late Miocene atmospheres of −6.0‰, we can adjust the C_3 endmembers of modern plants collected when $\delta^{13}C$ of CO_2 was close to −8.0‰ by +2‰ such that C_3 plant endmember values would shift from −20‰ and −35‰ to −18‰ and −33‰ (Cerling and Harris, 1999; Tipple and Pagani, 2007). Therefore we have high confidence that the Miocene grass fossil carbon isotopic value of ~ −25‰ indicates these grasses used the C_3 pathway.

Despite the low total organic carbon content, we infer that the organic carbon is primary. Any surfaces exposed to potential contamination were cut away. The stems were isolated from the rock matrix by dissolving the matrix in dilute HCl until bubbling stopped. In thin section, low temperature recrystallization is evident however this is not known to change the primary organic carbon content. Furthermore, any possible isotopic effects would shift the isotope value to more enriched values and given the more ^{13}C depleted, C_3-like values, we do not suspect any alteration post-deposition of the organic carbon content or organic carbon isotopic value. We speculate that the primary carbon was preserved in the cuticle and released after powdering the fossil stems.

5.3. Comparison of grass fossils from the Dove Spring Formation

5.3.1. Carbon isotopes

Grass fossils previously reported from the Dove Spring Formation were interpreted to use the C_4 photosynthetic pathway based on anatomical and isotopic evidence (Nambudiri et al., 1978; Tidwell and Nambudiri, 1989). One of the defining characteristics of these fossil grasses was the isotopically ^{13}C-enriched values (−13.7‰) (Nambudiri et al., 1978). However, the reported method of preparation in that paper used hydrofluoric acid to digest silicates – a method that may not have been sufficient to remove carbonates, which have a ^{13}C-enriched composition relative to organic matter. However in a subsequent paper

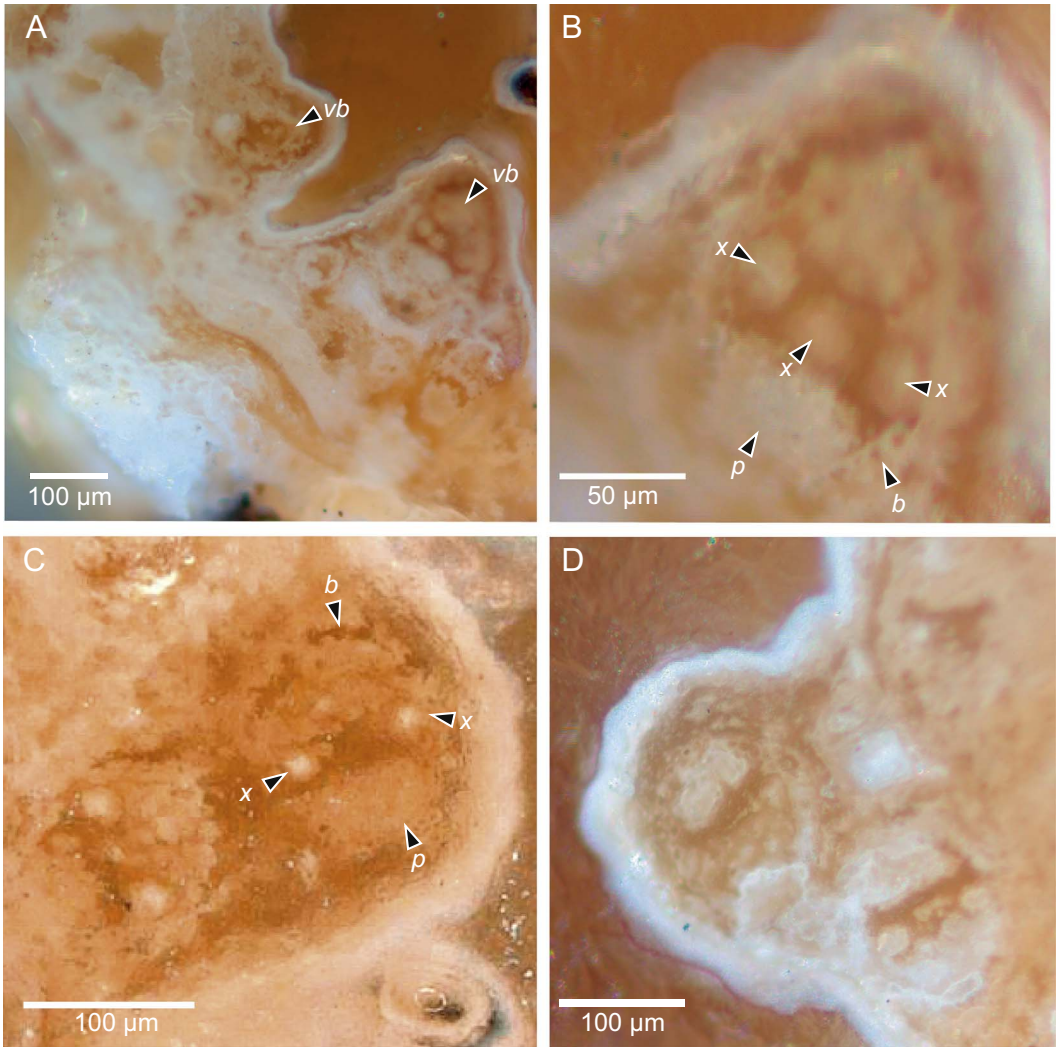

Fig. 5. Vascular bundles in cross-section of LACM 155204. (A) Vascular bundles protruding into the hollow culm. (B) A vascular bundles with bundle sheath cells (*b*), three metaxylem channels (*x*), and phloem (*p*). (C) Two vascular bundles with similar features as (B). (D) Three vascular bundles.

(Tidwell and Nambudiri, 1990), the authors of that study did use HCl, so it is possible that the method was incompletely reported and HCl may have been used to remove carbonates. HCl dissolution of carbonates requires extended heating for complete dissolution of recalcitrant carbonate (dolomite), and without this step, even a small amount of residual inorganic carbon could bias the organic carbon analyses toward heavier isotopic values (Whiteside et al., 2011). For example, in the samples presented in this study, given that the $\delta^{13}C$ of carbonates are ~ − 4‰ and the small organic carbon content, as little as 0.0005% of recalcitrant carbonate could have produced C_4-like values. A second concern with the previous study is the use of HF, which is known to alter organic matter resulting in increased variance of the true organic carbon isotope value (Barral et al., 2015). We were unable to access the samples collected by the prior study to test the reproducibility of the C_4 designation based on the carbon isotopic composition in light of these new method developments as the fossil material was destructively sampled for the initial carbon isotopic analysis (Nambudiri et al., 1978; Tidwell and Nambudiri, 1989). Here we reported $\delta^{13}C_{org}$ values for our newly-collected samples using exclusively HCl and heat to temperatures that remove recalcitrant carbonate. We found the additional grass fossils we recovered from the Dove Spring Formation all conclusively used the C_3 photosynthetic pathway.

5.3.2. Anatomy

All LACM fossils in this study have large vascular bundles within the culm that likely provided structural support for the stem. In general, vascular bundles used for photosynthesis were not abundantly preserved, as they are likely to degrade faster than the more lignified internal bundles. LACM 155204 has better preservation than LACM 160024, 160025, and 160026. This is evident as only structures that likely contain lignin, a more resistant biomolecule, were preserved including a prominent midrib and large vascular bundles that likely served as structural support in LACM 160024–26. In LACM 155204, additional structures are preserved including smaller vascular bundles within the leaf sheath. These vascular bundles are separated by 300 µm and are > 5 cells apart (Fig. 4D). This interveinal spacing is suggestive of C_3 photosynthesis. Cells with the positional landmarks of bundle sheath cells have diameters in the 20 µm range, overlapping the values reported for both C_3 and C_4 members of the PACMAD clade (Christin et al., 2013). Thus, without preservation of more detailed structure such as chloroplasts, it is not possible to distinguish C_4 from C_3 on bundle sheath cell diameter alone. Taken together, our results suggest that this fossil is a C_3. The anatomical features of LACM 160024, 160,025, and 160,026 are taphonomically limited, however the organic carbon value is in the C_3 isotopic range. Therefore, we infer that both fossils are indicative of C_3 plants.

The best preserved, LACM 155204 differs from the previously

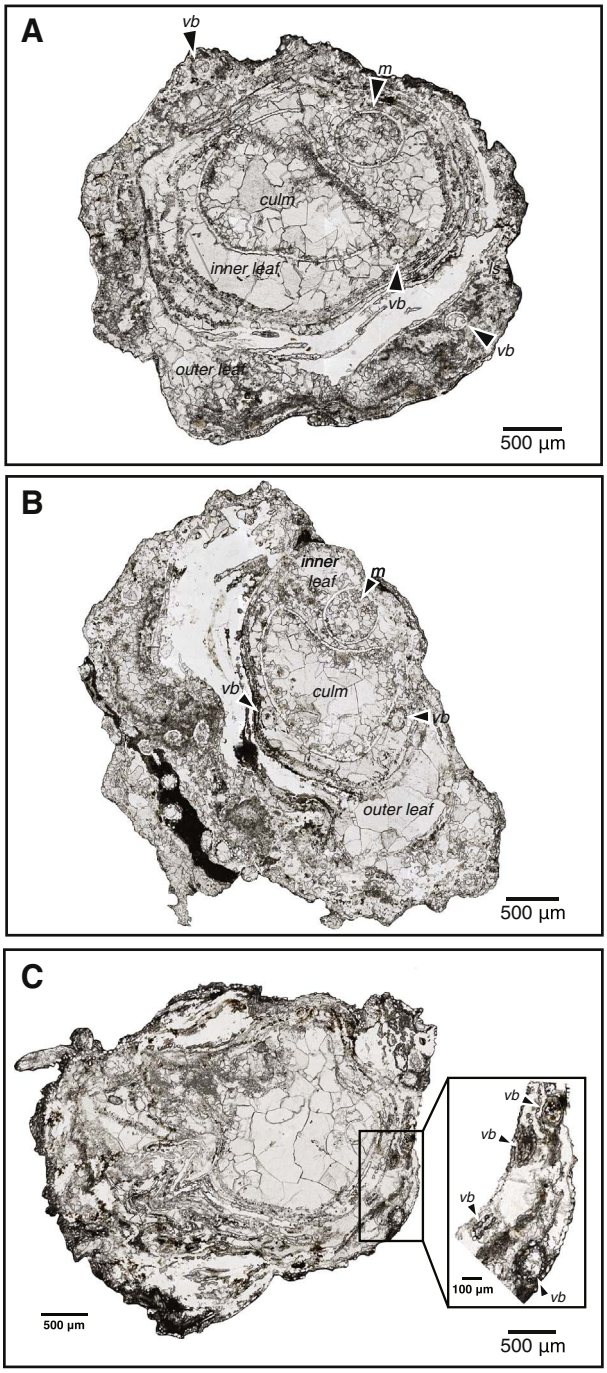

Fig. 6. Thin cross-section images of Miocene grass shoot fossils (A) LACM 160026, (B) LACM 160025, and (C) LACM 160024. Arrows point to vascular bundles (*vb*) and the large midvein (*m*) found within the innermost and outermost leaves that are arranged concentrically around the central culm in cross-section. The inset box in C enlarges two adjacent leaf sheaths that surround the central culm and highlight a larger vascular bundle with two vascular bundle sheaths including an inner mestome sheath and an outer parenchymatous bundle sheath.

Table 1
Carbon isotopic composition of fossil material and matrix material from the same hand sample that the thin section images (LACM 160024-LACM 160026) were taken.

Samples	$\delta^{13}C$ (‰)	Std. Dev. (‰)	*n*
Grass fossil	− 24.4	0.03	2
Matrix TOC	− 27.3	0.42	3
Matrix TIC	− 3.79	0.05	3

reported 'C_4' grass fossil, *Tomlinsonia thomassonii* from the late Miocene strata of the Dove Spring Formation in that the culm of LACM 155204 is hollow and larger (diameter up to 1.8 mm), whereas the culm of *T. thomassonii* is solid and smaller (diameter up to 200 µm). The organization of leaf sheath and blade tissues in *T. thomassonii* is similar to LACM 155204, with vascular bundles embedded in mesophyll tissues. Details of vascular bundles, including multiple-layered sclerified bundle sheaths, and mesophyll, including cells that radiate from the veins, are particularly well preserved in *T. thomassonii* (Tidwell and Nambudiri, 1989). Published illustrations of *T. thomassonii* leaf blades differ from other C_4 grasses in thick leaf blades and in substantial volumes of mesophyll tissue associated with each vein. The physiological requirement for a short diffusion pathway for C_4 metabolites is manifested anatomically not only by close vein spacing, but also by reduced volumes of mesophyll tissue associated with each vein and thin leaves, features not seen in *T. thomassonii* (Dengler et al., 1994). These anatomical features lead us to suggest caution in identifying *T. thomassonii* as C_4.

5.4. Miocene-age paleoecological reconstructions from the present day Mojave Desert

From the Dove Spring Formation, additional silicified plant remains are limited to petrified wood assemblages and further evidence of other C_4 clades were not found. Tree species characteristic of low elevations in close proximity of streams includes palms (*Palmoxylon mohavensis*) and locusts (*Robinia alexanderi*), whereas oaks (*Quercus ricardensis*), pines (*Pinus kelloggi*) and cypress (*Cupressus*) trees could be found on upstream slopes farther away from the streambeds (Webber, 1933). Fluvial and lacustrine sediment facies suggest a lake environment with braided streams (Whistler et al., 2009). The robust size of the plant fossils suggests that they grew in a wet, marshy environment, consistent with the paleoenvironmental interpretation of the lithology. While it is possible for C_4 grasses to be associated with aerially restricted groundwater fed springs with water available in summer months or around saline lakes, we confirmed that these recently analyzed grasses used the C_3 photosynthetic pathway.

The presence of widespread grasses at this locality can be inferred from the preservation of herbivores throughout the Dove Spring Formation. Herbivore tooth enamel records the availability and/or uptake of dominantly C_3 resources (Bowman et al., 2017). Taxa including grazers, browsers and mixed feeders have enamel values ranging from − 13.3 to − 6.7‰ with an average value of − 10.1‰ (Bowman et al., 2017). Enamel values greater than − 8.0‰ only accounted for 1% of the total individuals sampled. A $\delta^{13}C$ enamel value of − 8.0‰ is considered the modern cut off for a diet of C_3 plants (Feranec and Pagnac, 2013), however this would shift to − 6‰ considering the more ^{13}C enriched atmosphere of the Miocene (Bowman et al., 2017). Therefore, the possibility of the consumption of C_4 plants is unlikely given the more ^{13}C enriched Miocene atmospheres at this time (Bowman et al., 2017). Overall grazers had the most positive values, and these values may reflect water stressed C_3 plants. Serial sampling of the herbivore teeth did not reveal a seasonal signal in $\delta^{13}C$ indicating a consistent diet of C_3 resources among the individuals sampled (Bowman et al., 2017). Herbivore diets indicate that C_3 grasses were a readily available resource on the landscape, and C_4 grasses were either absent or not exploited by the wide range of herbivores sampled from the Dove Spring Formation.

Mid-Miocene age (14–13.4 Myr) herbivore tooth enamel from the Barstow Formation was interpreted to support an early C_4 expansion in the Mojave region (Feranec and Pagnac, 2013). While the diets of most browsers and grazers including antilocapridae, camelidae, and gomphotheriidae consisted of pure C_3 resources, the horses, equids, had diets slightly more enriched in ^{13}C (− 7.8 ± 0.8‰) with values up to − 6.2‰ (Feranec and Pagnac, 2013). The authors applied a linear mixing model assuming a C_3 end member of − 8‰ to estimate the

percentage of C_4 plants consumed by equidae. Using this approach, they approximated that up to 18% of C_4 plants were included in the diets of some ungulates. However, linear mixing models fail to account for the large range of $\delta^{13}C$ values of C_3 plants, and propagated error associated with the C_3 isotopic range (2.3‰) and uncertainty associated with $\delta^{13}C$ CO_2 estimates (0.2‰) translates into an error estimate of ± 20% C_4. Therefore, we cannot assume with confidence that C_4 was incorporated in equidae diets from the Barstow Formation during the upper Miocene. Taken together, late Miocene herbivores from the Mojave Desert likely did not exploit C_4 resources either due to the absence of C_4 on the landscape or a C_3 dietary preference of all the taxa sampled.

5.5. North American grassland expansion

The development of North American grasslands occurred in two phases (Edwards et al., 2010; Strömberg, 2011). The late Oligocene and early Miocene (ca. 25–20 Myr) witnessed the initial spread of C_3 grasslands and open woodlands (Strömberg, 2011; Strömberg, 2004). Early evidence of the presence, but not dominance, of C_4 plants is observed in the early-middle Miocene. By 19 Ma, phytoliths indicative of C_4 Chloridoideae species are present in grassland assemblages from the Great Plains (Strömberg, 2005). Leaf wax $\delta^{13}C$ records from the Gulf of Mexico document a peak in ^{13}C-enriched $\delta^{13}C$ values during the Middle Miocene Climatic Optimum ca. 15 Ma (Tipple and Pagani, 2010). Soil carbonates from the Great Plains also document a corresponding increase in $\delta^{13}C$ values (Fox and Koch, 2003). Evidence of an early C_4 expansion is not regionally uniform, and tooth enamel records from California do not capture a significant increase in C_4 plants in mid-Miocene to late Miocene strata (Bowman et al., 2017; Feranec and Pagnac, 2013). Beginning in the late Miocene through to the Pliocene, the replacement of C_3 grasslands and dominance of C_4 grasslands occurs in several regions. In the Great Plains, C_4 grasses generally increased initially as a mixed C_3/C_4 grasslands by 5.5 Ma and then to proportions > 80% by 2 Ma based on phytolith assemblages and carbon isotopes of phytoliths (McInerney et al., 2011; Strömberg and McInerney, 2011). In the Pliocene, carbon isotopes in soil carbonates records document the widespread abundance of C_4 vegetation in the Great Plains, Arizona and New Mexico (Fox and Koch, 2003; Mack et al., 1994; Wang et al., 1993).

The grass fossil record accompanying this history of grasslands remains sparse. Here we report C_3 grass fossils recovered from one of the key C_4 grass fossil localities. To date, C_4 grass macrofossils have only been recovered from the late Miocene despite earlier origins estimated in the Early Oligocene (~30–32 Myr). Identifying grass fossils with sufficient anatomical and organic carbon preservation for C_3 or C_4 identification is a high priority to secure our reconstructions of grass evolution, C_4 origins and paleoecological reconstructions. In light of the findings presented here, we cannot corroborate previous reports of the oldest C_4 grass fossils from this region. Based on a careful reading of the published reports, in those prior studies, carbon isotopic analysis included HF-digestion methods that may not have removed carbonate from the sample, and any remnant carbonate contamination would erroneously bias the carbon isotopic value toward C_4-like values. We revisited the Dove Spring Formation to collect additional fossils, and for all the samples we collected, the results definitively indicate the use of the C_3 photosynthetic pathway. We have been unable to obtain additional, corroborative evidence for C_4 grasses beyond the original publication (Nambudiri et al., 1978; Tidwell and Nambudiri, 1989).

6. Conclusions

In this study, we revisited the oldest known locality of C_4 grasses and collected additional grass fossils from two new stratigraphic positions within the late Miocene-age Dove Spring Formation in southern California. Anatomical descriptions based on microscopy of grass stems in cross section and organic carbon isotopic compositions after high-temperature carbonate removal provides conclusive evidence that these fossils are C_3 grasses and no new C_4 grass fossils were found. This finding supports other studies that have found that C_3 grasses were widespread throughout the region, and C_4 grasses had limited occurrence, if present at all. In closing we highlight the exceedingly sparse grass macro-fossil record despite the ecological and climatic importance of the evolution of C_4 grasslands.

Acknowledgments

These samples were collected under the collection permit of Xiaoming Wang, with assistance from Dave Whistler, Gary Takeuchi, and Mark Faull. We would like to thank two anonymous reviewers whose comments improved the manuscript. We thank Thure Cerling for drawing our attention to this interesting research question and locality. We thank Josh West and Will Berelson for access to facilities for high temperature decarbonation and carbon isotopic analyses. We thank Nick Rollins, Yadira Ibarra, Dylan Wilmeth and Joyce Yager for laboratory assistance. This work was supported by funding from the University of Southern California to SF and HL. This research did not receive any specific grant from funding agencies in the public, commercial, or not-for-profit sectors.

References

Barral, A., Lécuyer, C., Gomez, B., Fourel, F., Daviero-Gomez, V., 2015. Effects of chemical preparation protocols on $\delta^{13}C$ of plant fossil samples. Palaeogeogr. Palaeoclimatol. Palaeoecol. 438, 267–276. http://dx.doi.org/10.1016/j.palaeo.2015.08.016.

Bonnichsen, B., Leeman, W.P., Honjo, N., McIntosh, W.C., Godchaux, M.M., 2008. Miocene silicic volcanism in southwestern Idaho: geochronology, geochemistry, and evolution of the central Snake River Plain. Bull. Volcanol. 70, 315–342. http://dx.doi.org/10.1007/s00445-007-0141-6.

Bowes, G., 2011. Single-cell C_4 photosynthesis in aquatic plants. In: Raghavendra, A.S., Sage, R.F. (Eds.), C4 Photosynthesis and Related CO2 Concentrating Mechanisms, Advances in Photosynthesis. Springer, Dordrecht, pp. 63–80.

Bowman, C.N., Wang, Y., Wang, X., Takeuchi, G.T., Faull, M., Whistler, D.P., Kish, S., 2017. Pieces of the puzzle: lack of significant C_4 in the late Miocene of southern California. Palaeogeogr. Palaeoclimatol. Palaeoecol. 475, 70–79. http://dx.doi.org/10.1016/j.palaeo.2017.03.008.

Brodie, C.R., Leng, M.J., Casford, J.S.L., Kendrick, C.P., Lloyd, J.M., Yongqiang, Z., Bird, M.I., 2011. Evidence for bias in C and N concentrations and $\delta^{13}C$ composition of terrestrial and aquatic organic materials due to pre-analysis acid preparation methods. Chem. Geol. 282, 67–83. http://dx.doi.org/10.1016/j.chemgeo.2011.01.007.

Brown, W.V., 1975. Variations in anatomy, associations, and origins of Kranz tissue. Am. J. Bot. 62, 395–402.

Burbank, D.W., Whistler, D.P., 1987. Temporally constrained tectonic rotations derived from magnetostratigiraphic data: implications for the initiation of the Garlock fault, California. Geology 15, 1172–1175.

Cerling, T.E., 1999. Paleorecords of C_4 plants and ecosystems. In: Sage, R.F., Monson, R.K. (Eds.), C_4 Plant Biology. Academic Press, San Diego, CA, USA, pp. 445–469.

Cerling, T.E., Harris, J.M., 1999. Carbon isotope fractionation between diet and bioapatite in ungulate mammals and implications for ecological and paleoecological studies. Oecologia 120, 347–363.

Cerling, T.E., Quade, J., Ambrose, S.H., Sikes, N.E., 1991. Fossil soils, grasses, and carbon isotopes from Fort Ternan, Kenya: grassland or woodland? J. Hum. Evol. 21, 295–306.

Christin, P.-A., Osborne, C.P., 2014. The evolutionary ecology of C_4 plants. New Phytol. 204, 765–781. http://dx.doi.org/10.1111/nph.13033.

Christin, P.-A., Besnard, G., Samaritani, E., Duvall, M.R., Hodkinson, T.R., Savolainen, V., Salamin, N., 2008. Oligocene CO_2 decline promoted C_4 photosynthesis in grasses. Curr. Biol. 18, 37–43. http://dx.doi.org/10.1016/j.cub.2007.11.058.

Christin, P.-A., Osborne, C.P., Chatelet, D.S., Columbus, J.T., Besnard, G., Hodkinson, T.R., Garrison, L.M., Vorontsova, M.S., Edwards, E.J., 2013. Anatomical enablers and the evolution of C_4 photosynthesis in grasses. Proc. Natl. Acad. Sci. 110, 1381–1386. http://dx.doi.org/10.1073/pnas.1216777110/-/DCSupplemental/sd01.xls.

Christin, P.A., Spriggs, E., Osborne, C.P., Strömberg, C.A.E., Salamin, N., Edwards, E.J., 2014. Molecular dating, evolutionary rates, and the age of the grasses. Syst. Biol. 63, 153–165. http://dx.doi.org/10.1093/sysbio/syt072.

Cox, B.F., Diggles, M.F., 1986. Geologic map of the El Paso Mountains wilderness study area, Kern County, California. In: U. S. Geological Survey Miscellaneous Field Studies Map.

Dengler, N.G., Nelson, T., 1998. Leaf structure and development in C_4 plants. In: Sage, R.F., Monson, R. (Eds.), C_4 Plant Biology. Academic Press.

Dengler, N.G., Dengler, R.E., Donnelly, P.M., Hattersley, P.W., 1994. Quantitative leaf anatomy of C_3 and C_4 grasses (Poaceae): bundle sheath and mesophyll surface area relationships. Ann. Bot. 73, 241–255.

Dibblee Jr., T.W., 1952. Geology of the Saltdale quadrangle, California. Calif. Div. Min. Bull. 160, 5–43.

Dugas, D.P., Retallack, G.J., 1993. Middle Miocene fossil grasses from Fort Ternan, Kenya.

J. Paleontol. 67, 113–128.
Edwards, G.E., Furbank, R.T., Hatch, M.D., Osmond, C.B., 2001. What does it take to be C_4? Lessons from the evolution of C_4 photosynthesis. Plant Physiol. 125, 46–49.
Edwards, E.J., Osborne, C.P., Strömberg, C.A.E., Smith, S.A., C4 Grasses Consortium, Bond, W.J., Christin, P.A., Cousins, A.B., Duvall, M.R., Fox, D.L., Freckleton, R.P., Ghannoum, O., Hartwell, J., Huang, Y., Janis, C.M., Keeley, J.E., Kellogg, E.A., Knapp, A.K., Leakey, A.D.B., Nelson, D.M., Saarela, J.M., Sage, R.F., Sala, O.E., Salamin, N., Still, C.J., Tipple, B., 2010. The origins of C_4 grasslands: integrating evolutionary and ecosystem science. Science 328, 587–591. http://dx.doi.org/10.1126/science.1177216.
Ehleringer, J.R., Cerling, T.E., Helliker, B.R., 1997. C_4 photosynthesis, atmospheric CO_2, and climate. Oecologia 112, 285–299.
Farquhar, G.D., Ehleringer, J.R., Hubick, K.T., 1989. Carbon isotope discrimination and photosynthesis. Annu. Rev. Plant Biol. 40, 503–537.
Feranec, R.S., Pagnac, D., 2013. Stable carbon isotope evidence for the abundance of C_4 plants in the middle Miocene of southern California. Palaeogeogr. Palaeoclimatol. Palaeoecol. 388, 42–47. http://dx.doi.org/10.1016/j.palaeo.2013.07.022.
Fox, D.L., Koch, P.L., 2003. Tertiary history of C_4 biomass in the Great Plains, USA. Geology 31, 809–812.
Freitag, H., Stichler, W., 2000. A remarkable new leaf type with unusual photosynthetic tissue in a central Asiatic genus of Chenopodiaceae. Plant Biol. 2, 154–160.
Friedli, H., Lotscher, H., Oeschger, H., Siegenthaler, U., Stauffer, B., 1986. Ice core record of the $^{13}C/^{12}C$ ratio of atmospheric CO_2 in the past two centuries. Nature 324, 1–2.
Galy, V., Bouchez, J., France Lanord, C., 2007. Determination of total organic carbon content and $\delta^{13}C$ in carbonate-rich detrital sediments. Geostand. Geoanal. Res. 31, 199–207.
Gibson, D.J., 2009. Grasses and Grassland Ecology. Oxford University Press, Oxford, UK.
Hatch, M.D., 1987. C_4 photosynthesis: a unique blend of modified biochemistry, anatomy and ultrastructure. Biochim. Biophys. Acta 895, 81–106.
Hattersley, P.W., 1984. Characterization of C_4 type leaf anatomy in grasses (Poaceae). Mesophyll: bundle sheath area ratios. Ann. Bot. 2, 163–180.
Hattersley, P.W., Watson, L., 1975. Anatomical parameters for predicting photosynthetic pathways of grass leaves: the 'maximum lateral cell count' and the 'maximum cells distant count. Phytomorphology 25, 325–333.
Kadereit, G., Borsch, T., Weising, K., Freitag, H., 2003. Phylogeny of Amaranthaceae and Chenopodiaceae and the evolution of C_4 photosynthesis. Int. J. Plant Sci. 164, 959–986. http://dx.doi.org/10.1086/378649.
Keeling, C.D., Piper, S.C., Bacastow, R.B., Wahlen, M., Whorf, T.P., Martin, H., Meijer, H.A., 2001. Exchanges of Atmospheric co_2 and $^{13}co_2$ with the Terrestrial Biosphere and Oceans from 1978 to 2000. I. Global Aspects (no. 01–06), SIO Reference.
Leegood, R.C., 2002. C_4 photosynthesis: principles of CO_2 concentration and prospects for its introduction into C_3 plants. J. Exp. Bot. 53, 581–590.
Loomis, D.P., Burbank, D.W., 1988. The stratigraphic evolution of the El Paso basin, southern California: implications for the Miocene development of the Garlock fault and uplift of the Sierra Nevada. Geol. Soc. Am. Bull. 100, 12–28.
Lundgren, M.R., Osborne, C.P., Christin, P.-A., 2014. Deconstructing Kranz anatomy to understand C_4 evolution. J. Exp. Bot. 65, 3357–3369. http://dx.doi.org/10.1093/jxb/eru186.
Mack, G.H., Cole, D.R., James, W.C., Giordano, T.H., Salyards, S.L., 1994. Stable oxygen and carbon isotopes of pedogenic carbonate as indicators of Plio-Pleistocene paleoclimate in the southern Rio Grande Rift, south-central New Mexico. Am. J. Sci. 294, 621–640.
McInerney, F.A., Strömberg, C., White, J., 2011. The Neogene transition from C_3 to C_4 grasslands in North America: stable carbon isotope ratios of fossil phytoliths. Paleobiology 37, 23–49.
Merriam, J.C., 1919. Tertiary Mammalian Faunas of the Mojave Desert. University of California Publications, Department of Geology, Bulletin.
Monastero, F.C., Sabin, A.E., Walker, J.D., 1997. Evidence for post–early Miocene initiation of movement on the Garlock fault from offset of the Cudahy Camp Formation, east-central California. Geology 25, 247–250.
Muhaidat, R., Sage, R.F., Dengler, N.G., 2007. Diversity of Kranz anatomy and biochemistry in C_4 eudicots. Am. J. Bot. 94, 362–381.
Nambudiri, E., Tidwell, W.D., Smith, B.N., Hebbert, N.P., 1978. A C_4 plant from the Pliocene. Nature 276, 816–817.
Ogle, K., 2003. Implications of interveinal distance for quantum yield in C_4 grasses: a modeling and meta-analysis. Oecologia 136, 532–542. http://dx.doi.org/10.1007/s00442-003-1308-2.
Passey, B.H., Cerling, T.E., Perkins, M.E., Voorhies, M.R., Harris, J.M., Tucker, S.T., 2002. Environmental change in the Great Plains: an isotopic record from fossil horses. J. Geol. 110, 123–140.
Perkins, M.E., Nash, B.P., 2002. Explosive silicic volcanism of the Yellowstone hotspot: the ash fall tuff record. Geol. Soc. Am. Bull. 114, 367–381.
Perkins, M.E., Brown, F.H., Nash, W.P., McIntosh, W.C., Williams, S.K., 1998. Sequence, age, and source of silicic fallout tuffs in middle to late Miocene basins of the northern Basin and Range province. Geol. Soc. Am. Bull. 110, 344–360.
Prasad, V., Strömberg, C., Leaché, A.D., Samant, B., Patnaik, R., Tang, L., Mohabey, D.M., Ge, S., Sahni, A., 2011. Late Cretaceous origin of the rice tribe provides evidence for early diversification in Poaceae. Nat. Commun. 2, 1–9. http://dx.doi.org/10.1038/ncomms1482.
Retallack, G.J., 1990. Soils of the Past: An Introduction to Paleopedology. Hyman, Boston, Ma.
Retallack, G.J., 1992. Middle Miocene fossil plants from Fort Ternan (Kenya) and evolution of African grasslands. Paleobiology 18, 383–400.
Retallack, G.J., Dugas, D.P., Bestland, E.A., 1990. Fossil soils and grasses of a middle Miocene east African grassland. Science 247, 1325–1328.
Sack, L., Scoffoni, C., 2013. Leaf venation: structure, function, development, evolution, ecology and applications in the past, present and future. New Phytol. 198, 983–1000. http://dx.doi.org/10.1111/j.1365-3040.2005.01448.x.
Sack, L., Scoffoni, C., McKown, A.D., Frole, K., Rawls, M., Havran, J.C., Tran, H., Tran, T., 2012. Developmentally based scaling of leaf venation architecture explains global ecological patterns. Nat. Commun. 3, 1–10. http://dx.doi.org/10.1038/ncomms1835.
Sage, R.F., 2016. A portrait of the C_4 photosynthetic family on the 50th anniversary of its discovery: species number, evolutionary lineages, and hall of fame. J. Exp. Bot. 1–18. http://dx.doi.org/10.1093/jxb/erw156.
Sage, R.F., Christin, P.A., Edwards, E.J., 2011. The C_4 plant lineages of planet Earth. J. Exp. Bot. 62, 3155–3169. http://dx.doi.org/10.1093/jxb/err048.
Sage, R.F., Sage, T.L., Kocacinar, F., 2012. Photorespiration and the evolution of C_4 photosynthesis. Annu. Rev. Plant Biol. 63, 19–47. http://dx.doi.org/10.1146/annurev-arplant-042811-105511.
Sinha, N.R., Kellogg, E.A., 1996. Parallelism and diversity in multiple origins of C_4 photosynthesis in the grass family. Am. J. Bot. 83, 1458–1470.
Smith, E.I., Sánchez, A., Keenan, D.L., 2002. Stratigraphy and geochemistry of volcanic rocks in the Lava Mountains, California: implications for the Miocene development of the Garlock fault. In: Glazner, A.F., Walker, J.D., Bartley, J.M. (Eds.), Geologic Evolution of the Mojave Desert and Southwestern Basin and Range. Geological Society of America Memoir, pp. 151–160.
Strömberg, Caroline, 2004. Using phytolith assemblages to reconstruct the origin and spread of grass-dominated habitats in the great plains of North America during the late Eocene to early Miocene. Palaeogeogr. Palaeoclimatol. Palaeoecol. 207, 239–275. http://dx.doi.org/10.1016/j.palaeo.2003.09.028.
Strömberg, C.A.E., 2005. Decoupled taxonomic radiation and ecological expansion of open-habitat grasses in the Cenozoic of North America. Proc. Natl. Acad. Sci. 102, 11980–11984.
Strömberg, C.A.E., 2011. Evolution of grasses and grassland ecosystems. Annu. Rev. Earth Planet. Sci. 39, 517–544. http://dx.doi.org/10.1146/annurev-earth-040809-152402.
Strömberg, Caroline A.E., McInerney, F.A., 2011. The Neogene transition from C_3 to C_4 grasslands in North America: assemblage analysis of fossil phytoliths. Paleobiology 37, 50–71. http://dx.doi.org/10.1666/09067.s1.
Tedford, R.H., Skinner, M.F., Fields, R.W., Rensberger, J.M., Galusha, T., Taylor, B.E., MacDonald, J.R., Webb, S.D., Whistler, D.P., 1987. Faunal succession and biochronology of the Arikareean through Hemphillian interval (late Oligocene through earliest Pliocene Epochs) in North America. In: Woodburne, M.O. (Ed.), Cenozoic Mammals of North America. University of California Press, Berkeley, California, pp. 153–210.
Thomasson, J.R., Nelson, M.E., Zakrzewski, R.J., 1986. A fossil grass (Gramineae: Chloridoideae) from the Miocene with Kranz anatomy. Science 233, 876–878.
Tidwell, W.D., Nambudiri, E., 1989. *Tomlisonia thomassonii*, gen. Et sp. Nov., a permineralized grass from the upper Miocene Ricardo Formation, California. Rev. Palaeobot. Palynol. 60, 165–177.
Tidwell, W.D., Nambudiri, E., 1990. *Tomlinsonia stichkania* sp. Nov., a permineralized grass from the Pliocene to (?) Pleistocene China Ranch beds in Sperry Wash, California. Bot. Gaz. 151, 263–274.
Tipple, B.J., Pagani, M., 2007. The early origins of terrestrial C_4 photosynthesis. Annu. Rev. Earth Planet. Sci. 35, 435–461. http://dx.doi.org/10.1146/annurev.earth.35.031306.140150.
Tipple, B.J., Pagani, M., 2010. A 35 Myr North American leaf-wax compound-specific carbon and hydrogen isotope record: implications for C_4 grasslands and hydrologic cycle dynamics. Earth Planet. Sci. Lett. 299, 250–262. http://dx.doi.org/10.1016/j.epsl.2010.09.006.
Tipple, B.J., Meyers, S.R., Pagani, M., 2010. Carbon isotope ratio of Cenozoic CO_2: a comparative evaluation of available geochemical proxies. Paleoceanography 25 (PA3202). https://doi.org/10.1029/2009PA001851.
Vicentini, A., Barber, J.C., Aliscioni, S.S., Giussani, L.M., Kellogg, E.A., 2008. The age of the grasses and clusters of origins of C_4 photosynthesis. Glob. Chang. Biol. 14, 1–15. http://dx.doi.org/10.1111/j.1365-2486.2008.01688.x.
Voznesenskaya, E.V., Franceschi, V.R., Kiirats, O., Freitag, H., Edwards, G.E., 2001. Kranz anatomy is not essential for terrestrial C_4 plant photosynthesis. Nature 414, 543–546.
Wang, Y., Cerling, T.E., Quade, J., Bowman, J.R., Smith, G.A., Lindsay, E.H., 1993. Stable isotopes of paleosols and fossil teeth as paleoecology and paleoclimate indicators: an example from the St. David Formation, Arizona. In: Swart, P.K., Lohmann, K.C., Mckenzie, J., Savin, S. (Eds.), Climate Change in Continental Isotopic Records. American Geophysical Union, Washington, D. C. http://dx.doi.org/10.1029/GM078p0241.
Ward, P.D., Garrison, G.H., Williford, K.H., Kring, D.A., Goodwin, D., Beattie, M.J., McRoberts, C.A., 2007. The organic carbon isotopic and paleontological record across the Triassic–Jurassic boundary at the candidate GSSP section at Ferguson Hill, Muller Canyon, Nevada, USA. Palaeogeogr. Palaeoclimatol. Palaeoecol. 244, 281–289. http://dx.doi.org/10.1016/j.palaeo.2006.06.042.
Webber, J.E., 1933. Woods from the Ricardo Pliocene of Last Chance Gulch, California. 412. Carnegie Institution of Washington Publications, pp. 113–134.
Whistler, D.P., Burbank, D.W., 1992. Miocene biostratigraphy and biochronology of the Dove Spring Formation, Mojave Desert, California, and characterization of the Clarendonian mammal age (late Miocene) in California. Geol. Soc. Am. Bull. 104, 644–658.
Whistler, D.P., Tedford, R.H., Takeuchi, G.T., Wang, X., Tseng, J.Z., Perkins, M.E., 2009. Revised Miocene Biostratigraphy and Biochronology of the Dove Spring Formation, Mojave Desert, California. Museum of Northern Arizona Bulletin.
Whiteside, J.H., Olsen, P.E., Eglinton, T.I., Cornet, B., McDonald, N.G., Huber, P., 2011. Pangean great lake paleoecology on the cusp of the end-Triassic extinction. Palaeogeogr. Palaeoclimatol. Palaeoecol. 301, 1–17. http://dx.doi.org/10.1016/j.palaeo.2010.11.025.
Wood, A.E.I., Chaney, R.W., Clark, J.M.S., Colbert, E.D., Jepsen, G.L., Reesdie, J.B., Stock, C., 1941. Nomenclature and correlation of the North American continental Tertiary. Geol. Soc. Am. Bull. 1–48.